Estimation of the Radiative Sky Cooling Potential through Meteorological Data: A Case Study in Tropical Climate

Irvin Merchant[1], *Miguel* Chen Austin[1,2] and *Dafni* Mora[1,2,*]

[1]Faculty of Mechanical Engineering, Universidad Tecnológica de Panamá, Panama City, Panama

[2]Centro de Estudios Multidisciplinarios de Ingeniería, Ciencia y Tecnología (CEMCIT-AIP), Panama City, Panama

Abstract. In search of thermal comfort, over the years, various techniques have been developed to adapt to the conditions of the enclosures, depending on the region and the activity carried out. Thus, this project seeks to evaluate the radiative sky cooling potential for various areas of Panama. This evaluation will be carried out by developing a simplified mathematical model based on meteorological data. An uncertainty-sensibility analysis of the model was also carried out to highlight the critical parameters. Radiative sky cooling systems have been shown to be susceptible to cloudiness and humidity. With a tropical climate, Panama is critical to consider these two variables when developing the simplified mathematical model. Another aspect to consider when estimating the cooling potential will be the hours of the day when there is no solar radiation.

1 Introduction

The search for thermal comfort and other needs (cold food chains, server cooling, etc.) in recent years has led to the increasing use of air conditioning. Currently, cooling systems collectively account for 17% of the electricity used worldwide, representing 8% of greenhouse gas emissions. By 2050, it is predicted that total energy consumption for these systems could increase by six times the current value [1].

The constant use of air conditioning systems helps to satisfy thermal comfort in hot countries, but at the same time increases greenhouse gas emissions, contributing to global warming, and this will lead to the need for a higher cooling load, or in other words, a higher capacity air conditioning system, thus creating an unfavorable feedback loop.

Reducing the energy consumed by buildings is of utmost importance. By harnessing nature's sustainable resources, energy consumption from fossil fuels can be significantly reduced. One of these sustainable resources is the possibility of radiation exchange with the sky [2]. An object will radiate energy to the sky, which acts as a heat sink, causing the body temperature to decrease. This thermal radiation is also known as longwave radiation and is defined as electromagnetic radiation of wavelengths from 8 to 13 μm and from 13.5 to 16 μm [3].

The practical use of radiative cooling has been exploited by cultures in the desert areas of the Middle East long before the physical principles behind such phenomenon were understood and quantified. Persian peoples were able to produce ice by exposing thin pools of water to the night sky on winter nights. With adobe walls, the ponds were protected from the prevailing winds, and through the loss of heat by radiation, the water was able to freeze even when the ambient temperature was above 0°C [4].

Radiative cooling systems function similarly to conventional solar water heaters but without their transparent covers. For the design of a radiative cooling system, environmental conditions affect the system's performance, such as ambient temperature, relative air humidity, and cloud cover, all of which have a significant effect on the system's thermal performance.

---

[*] Corresponding author: dafni.mora@utp.ac.pa

It is possible to supply up to 80% of the total annual cooling load of a residential building by radiative cooling in favorable climates [5]. There are two common options for cooling buildings by nighttime radiative cooling. The first method is to cool the building's thermal storage mass (usually a horizontal roof or roof water pool) directly at night and seal and insulate it during the day [5]. Hay and Yellott tested a rooftop pool with movable insulation for one year of passive air conditioning. They concluded that if the dew point temperature is low enough, the roof pond can meet the cooling demand of the building in summer without any external energy consumption [6].

The second method involves using a heat transfer medium (i.e., water or air) between a radiator and the building envelope. Ezekwe conducted experimental studies to show the potential of a radiative cooling system combined with a thermal storage tank. As a result, he built and tested a nighttime passive cooling system consisting of a near-black emitter (radiative plate), a series of heat pipe elements, and a cold storage tank. A cooling capacity of 628 kJ/m^2 per night was reported with a minimum achievable temperature difference of -7 °C, which can be used during the day to meet the cooling needs of the building [7].

Another potential application for radiative cooling is the dissipation of low-grade heat from power plants. Currently, most thermal power plants rely on water cooling technologies to remove low-grade heat from the plants. Olwi et al. conducted theoretical and experimental studies on the use of radiative cooling of a covered cooling pond to cool a power plant in hot and arid locations. They proposed a water pond covered by a radiator plate to cool hot water coming from a power plant condenser. An average radiative heat flux of 50 W/m^2 was measured for their experimental setup during the night. Finding an efficient dry cooling method is significant for solar thermal power plants [8].

Thus, this research aims to develop a simplified mathematical model for estimating radiative sky cooling potential from meteorological data of a given site. A case study is presented for a tropical climate in Panama City.

2 Methodology

2.1 Description of the case study

The cafeteria university building is located in Panama, Panama City (9°01'16"N 79°31'59"W) (Figure 1(a)). This region has a rainy tropical climate. Within the cafeteria building, the kitchen zone was selected as the studied zone, since large amount of radiation heat transfer is exchanged due to the use of ovens, preheaters, bain-marie, and no air conditioner should be implemented to enhance comfort. This zone has a floor area of 37.06 m^2 and a volume of 111.18 m^3, with a total wall area of 73.22 m^2 (Figure 1(b)). The cafeteria has two roofs; the first (from the bottom up) is a sandwich roof. Its configuration is 3 cm thick of expanded polyurethane with zinc sheets on the interior and exterior. The second roof is a zinc sheet. A 3D model of the building was developed in DesignBuilder software to assess the thermal behavior of the studied zone in terms of air temperature, mean radiant temperature, and internal heat gains.
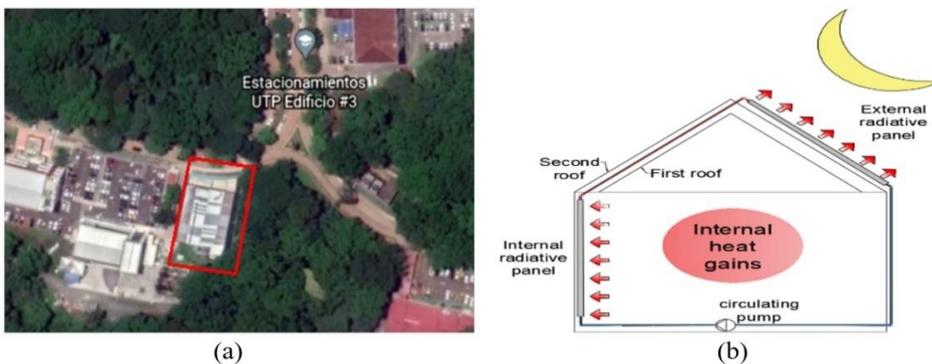
Fig. 1. Case of study: (a) Geographical location of the cafeteria and (b) schematic of the radiative cooling system.

2.2 Radiative cooling system

A panel system with water recirculation was developed in order to remove internal heat gains from the enclosure. In the study area, panels were placed, as shown in Figure 1(b), to cover the entire surface of the interior walls. The same number of panels was also placed on the ceiling.

The design of the nighttime radiative cooling system consists of external and internal radiative panels and a circulation pump (Figure 1(b)). This system aims to maintain the comfort temperature of the enclosure, and this will be achieved by nighttime radiation. The radiative panels inside have a rectangular duct (1 cm x 0.5 cm) embedded on an insulating base, allowing a greater contact of the fluid with the panel's surface (Figure 2(a)).
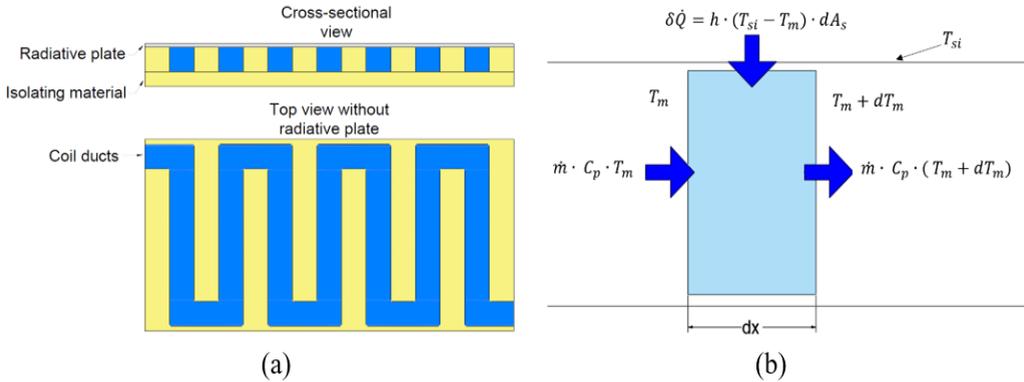
Fig. 2. Hydraulic system definition: (a) Top and cross-sectional view of the radiative panel and (b) thermal analysis for the fluid inside the stove coil.

The EES (Engineering Equation Solver) software was used to solve the model since the software already includes the properties of water, which facilitates its calculation and allows us to solve the systems of equations quickly. From the meteorological data of Panama, four days were chosen to be evaluated: the day with the highest ambient temperature and the day with the lowest temperature, and the days with the highest and lowest precipitation because their conditions are the most favorable unfavorable for the system.

The system model is based on an ideal heat exchange and consists of the equations presented below. First, a heat flow balance was performed on the panels inside the enclosure. This flow balance considers that the heat gained by the water passing through the panels is equal to the radiation and convection heat exchange experienced by the panel surface (equation (1)).

$$\dot{m} \cdot A_{mc} \cdot (T_{ei} - T_{ii}) = \varepsilon \cdot \sigma \cdot A_{mc} \cdot (T_{rm}^4 - T_{si}^4) + h_{ci} \cdot A_{mc} \cdot (T_{int} - T_{si}) \qquad (1)$$

where $\dot{m}$ is the mass flow of water through the panels. This mass flow has constant value of 0.125 kg/s. The area of the inner panel module A_{mc}, is 0.28 m^2 for each panel; there are 180 panels on the roof and inside enclosure (360 panels in total). The outlet and inlet temperatures to the inner coil T_{ei} and T_{ii}, respectively. The emissivity of the radiative panel ε (both internal and external), with a value of 0.9. The Stefan-Boltzmann constant σ with a value of 5.67x10^{-8} W/m^{2}K^4, the mean radiant temperature T_{rm}, the surface temperature of the inner panel T_{si}, the convective coefficient between the interior air and the panel h_{ci}, whose value is set to 2.152 W/m^{2}K it is obtained by simulation in DesignBuilder and the internal temperature of the enclosure T_{int}.

In order to obtain the water temperature at the outlet of the inner panel, a thermal analysis was performed on a longitudinal differential (dx) of the fluid inside the inner coil (Figure 2(b)).

As the fluid moves along with the coil, it will gain heat from the radiative plate. Therefore, employing a flow balance on dx equation (2) can be obtained, obtaining the temperature at the outlet of the inner coil (T_{ei}):

$$T_{ei} = T_{si} + (T_{ii} - T_{si}) \cdot exp\left(\frac{-h_{coil} \cdot A_{sc}}{\dot{m} \cdot cp}\right) \qquad (2)$$

where h_{coil} is the convective coefficient inside the coil. All heat gained in the enclosure panels ($\dot{Q}_{total\ enclosure}$) is transported to the ceiling through the system and evacuated on the ceiling panels, this is ideally represented:

$\dot{Q}_{total\ enclosure} = \dot{Q}_{total\ roof}$. To obtain the heat given up in the roof, another heat flux balance was performed on the exterior radiative panel, obtaining equation (3):

$$\dot{Q}_{total\ roof} = -\varepsilon \cdot \sigma \cdot A_{mt} \cdot \left[T_{st}^4 - \left(F \cdot T_{sky}^4 \right) \right] - h_{ce} \cdot A_{mt} \cdot (T_{st} - T_{ext}) \tag{3}$$

where T_{st} and T_{ext} are the surface temperatures of the exterior panel and the exterior air, respectively. F is the view factor of the exterior panel with respect to the sky; a value of one (1) is assumed here since no objects are blocking the panel's view towards the sky. A_{mt} is the area of the exterior panel module, h_{ce} is the external convection constant, it is obtained by $h_{ce} = (6.1 \cdot V_v) + 11.4$ [9], where V_v is the wind speed over the roof of the building in m/s.

Finally, T_{sky} is the sky temperature obtained by equation (4) [10]:

$$T_{sky} = \varepsilon_{sky}^{0.25} \cdot T_{ext} \tag{4}$$

where ε_{sky} is the emissivity of the sky (atmospheric) and T_{ext} is the outdoor temperature in K.

To obtain ε_{sky}, a model was used that contemplates cloudiness and is based on meteorological tapes, expressed in the equation (5)[10]:

$$\varepsilon_{sky} = \varepsilon_{csky} + (1 - \varepsilon_{csky}) \cdot F_{cl} \tag{5}$$

where F_{cl} is the cloudiness factor and ε_{csky} is the emissivity for a clear sky, which is obtained by equation (6) [10]:

$$\varepsilon_{csky} = 0.711 + 0.56 \cdot \left(\frac{T_{dp}}{100} \right) + 0.73 \cdot \left(\frac{T_{dp}}{100} \right)^2 + 0.013 \cdot cos\left(\frac{\pi \cdot t}{12} \right) + 0.00012 \cdot (P_{atm} - 1000) \tag{6}$$

where t is the time at which the emissivity is to be evaluated, T_{dp} is the dew point temperature and P_{atm} is atmospheric pressure, both at the time the emissivity is to be evaluated [10]. These correlations used to obtain T_{sky} were chosen because they contemplate the meteorological factors of the site where the radiative sky cooling potential is to be evaluated.

For this model, the following hypotheses were considered:
- Heat gains and losses were considered ideal for both the panels and the system.
- An average radiant temperature of 27°C was set for the room because there are considerable thermal loads for a university cafeteria kitchen.
- A constant comfort temperature (T_{int}) was set for the enclosure of 25°C.
- The properties of water change with respect to temperature. The water temperature as it leaves the roof panel (T_{ii}) is 25°C and a pressure 1 atm.
- The heat exchange between the fluid and the inner surface of the panel is perfect.
- The system pump works ideally.
- The same number of panels were used on the roof and enclosure, on the roof there is more space available.

Thus, the model was solved for the four days mentioned above, in which F_{cl} was varied from 0 to 1 with an increment of 0.1 for hours with no solar radiation (19:00 to 5:00).

2.3 Radiative cooling potential as a function of meteorological data

To estimate the radiative cooling potential of the site $\dot{Q}_{rad}$ was evaluated for the four days using equation (7) where values for T_{st} were assumed based on meteorological data.

$$\dot{Q}_{rad} = \varepsilon \cdot \sigma \cdot A_{mc} \cdot \left[T_{st}^4 - \left(F \cdot T_{sky}^4 \right) \right] \tag{7}$$

The F_{cl} values were grouped into four intervals: 0 to 0.2, 0.3 to 0.5, 0.6 to 0.8, and 0.9 to 1. A multiple linear regression was performed for each interval according to the most relevant parameters according to the sensitivity analysis: T_{sky} and T_{dp}. The obtained $\dot{Q}_{rad}$ values by the regression are confronted with the values of $\dot{Q}_{rad}$ from solving the system model (equations ((1))-(6)). Additionally, to obtain a simplified expression to determine ε_{csky}, a multiple linear regression was performed as a function of T_{dp} and P_{atm}.

3 Analysis of results and discussion

3.1 Radiative cooling potential as a function of meteorological data

When solving the model using EES, the behavior of the nocturnal cooling potential ($\dot{Q}_{rad}$) was appreciated in order to obtain the most relevant variables for the development of the simplified model. When evaluating $\dot{Q}_{rad}$ with respect to relative humidity, an inverse proportional trend was observed, with non-significant differences between minimum and maximum.

Moreover, $\dot{Q}_{rad}$ was evaluated with respect to F_{cl}. It was observed that as F_{cl} increases, the radiation by radiative cooling decreases along with the temperature difference between T_{st} and T_{sky}, as shown in Figure 3. This trend prevails for the four days and for all hours (for space reasons, it is only presented for the most favorable hour, 5:00). These trends demonstrate the relevance of F_{cl}; as it increases, the values of ε_{sky} and T_{sky} also increase, and thus, resulting in a decrease of $\dot{Q}_{rad}$.
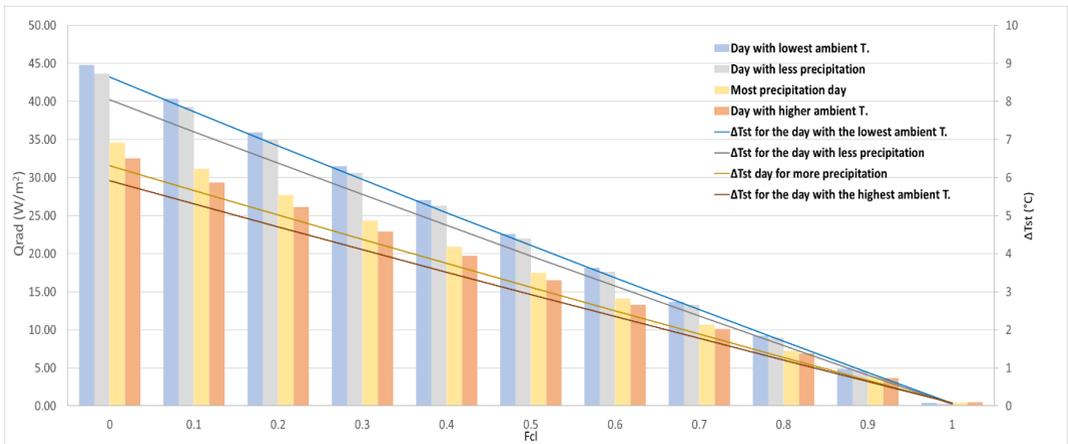
Fig. 3. Variation of nighttime potential $\dot{Q}_{rad}$ with respect to F_{cl} for 5:00.

By observing the behavior in Figure 3, the temperature difference between T_{st} and T_{sky} (ΔT_{st}). For each F_{cl} interval the average presented for ΔT_{st}. With the evaluation of the averages, F_{cl} d intervals were established where it was assumed that T_{st} would be equal to the addition of T_{sky} plus an adjusted $\Delta' T_{st}$ (Table 1). To obtain lower error percentages when evaluating the simplified model, an adjusted $\Delta' T_{st}$ was used after evaluating different values of ΔT_{st}, for each F_{cl} interval.

Table 1. Average and adjusted ΔT_{st} values for the F_{cl} intervals.

F_{cl} intervals	Average ΔT_{st} (°C)	Adjusted $\Delta' T_{st}$ (°C)
0 - 0.2	6.25	5.7
0.3 - 0.5	4.13	3.7
0.6 - 0.8	2.06	1.7
0.9 - 1	0.39	0.4

With the adjusted $\Delta' T_{st}$ the following regressions were obtained. For F_{cl} of 0 - 0.2 equation (8) was obtained:

$$\dot{Q}_{rad} = 94 \cdot \left(\frac{Tsky}{298.15}\right) + 0.92 \cdot \left(\frac{Tdp}{298.15}\right) - 61.51 \quad \left[\frac{W}{m^2}\right] \tag{8}$$

where the value 298.15 K is introduced to normalize the temperatures taking as reference the standard room temperature. Equation (8) presents a determination coefficient (R^2) of 0.9998, with a Mean Relative Error (MRE) of 20%. For F_{cl} of 0.3 - 0.5 equation (9) was obtained:

$$\dot{Q}_{rad} = 61.82 \cdot \left(\frac{Tsky}{298.15}\right) + 0.36 \cdot \left(\frac{Tdp}{298.15}\right) - 40.67 \quad \left[\frac{W}{m^2}\right] \tag{9}$$

with a R^2 de 0.9998 and a MRE of 20.5%. For F_{cl} of 0.6 - 0.8 equation (10) was obtained:

$$\dot{Q}_{rad} = 28.75 \cdot \left(\frac{Tsky}{298.15}\right) + 0.084 \cdot \left(\frac{Tdp}{298.15}\right) - 19.05 \quad \left[\frac{W}{m^2}\right] \tag{10}$$

With a R^2 of 0.9998 and a MRE of 26.8%. Figure 4 shows the MRE grouped for equations (8), (9), (10). It is possible to appreciate a higher occurrence in the MRE interval of 0 - 13.01%, indicating acceptable performance.
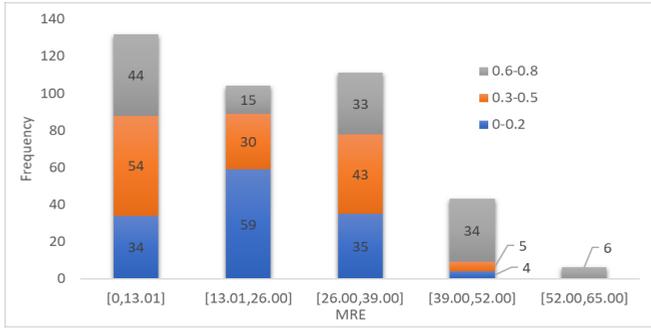
Fig. 4. Resulting MRE for each of the equations for $\dot{Q}_{rad}$: equation 8 (blue), equation 9 (orange), and equation 10 (gray).

A linear regression was not performed for the cases in which F_{cl} was 0.9 and 1 because when these values are maintained, the system does not operate satisfactorily, having occasions in which the roof radiative plates gain heat instead of losing.

Equation (11) corresponds to the simplification of ε_{csky} (equation (6)). Here, the value 101.325 kPa is introduced to normalize the atmospheric pressure taking as reference 1 atm, presenting a R^2 of 0.9671 and a MRE of 0.89%:

$$\varepsilon_{csky} = 2.85 \cdot \left(\frac{Tdp}{298.15}\right) + 1.11 \cdot \left(\frac{Patm}{1013.25}\right) - 3.04 \tag{11}$$

Finally, to estimate the radiative cooling potential of a site, based on meteorological data, the following set of equations is proposed (Table 2):

Table 2. Proposed simplify model to determine the radiative sky cooling potential from meteorological data.

Equations	Interval	MRE
$\dot{Q}_{rad} = 94 \cdot \left(\frac{Tsky}{298.15}\right) + 0.92 \cdot \left(\frac{Tdp}{298.15}\right) - 61.51$	$0 \leq Fcl \leq 0.2$	20%
$\dot{Q}_{rad} = 61.82 \cdot \left(\frac{Tsky}{298.15}\right) + 0.36 \cdot \left(\frac{Tdp}{298.15}\right) - 40.67$	$0.3 \leq Fcl \leq 0.5$	20.5%
$\dot{Q}_{rad} = 28.75 \cdot \left(\frac{Tsky}{298.15}\right) + 0.084 \cdot \left(\frac{Tdp}{298.15}\right) - 19.05$	$0.6 \leq Fcl \leq 0.8$	26.8%
$T_{sky} = \varepsilon_{sky}^{0.25} \cdot T_{ext}$	-	-
$\varepsilon_{sky} = \varepsilon_{csky} + \left(1 - \varepsilon_{csky}\right) \cdot F_{cl}$	-	-
$\varepsilon_{csky} = 2.85 \cdot \left(\frac{Tdp}{298.15}\right) + 1.11 \cdot \left(\frac{Patm}{1013.25}\right) - 3.04$	-	0.89%

3.2 Evaluation of the proposed model at different locations in Panama

The model was evaluated for three zones of Panama; Tocumen, Vista Hermosa, and the Canal Zone. For this evaluation, the meteorological data for 2019 was used, and a $F_{cl} = 0$ was established. Figure 5 shows the behavior of $\dot{Q}_{rad}$ for 2019. For this year, the arithmetic mean of $\dot{Q}_{rad}$ by zone was: 31.45 ± 0.50 W/m² for the Canal Zone, 31.60 ± 0.57 W/m² for Vista Hermosa, and 31.10 ± 0.47 W/m² for the Tocumen Airport; the average T_{ext} for the three zones was 26.56 ± 1.15 °C and T_{sky} for the three zones was 18.56 ± 1.47 °C. The

occurrence of $\dot{Q}_{rad}$ in the three zones and their respective average reflect favorable values, complying with the ranges foreseen in Figure 3.
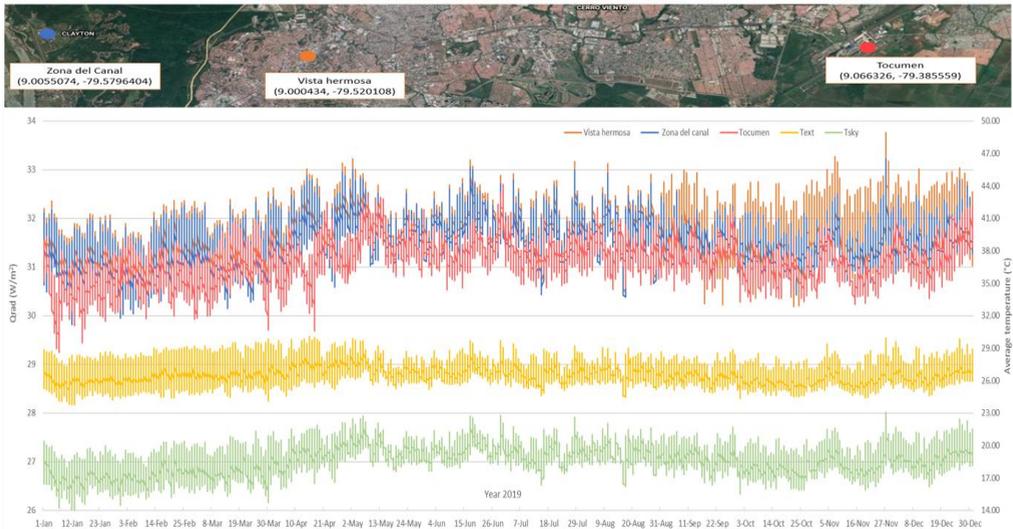
Fig. 5. $\dot{Q}_{rad}$ assessment in different locations within Panama using meteorological data from 2019.

The analysis of results and the evaluation of the methodological approach helped summarized the following limitations:

- The hypotheses contemplated in the modeling of the hydraulic system (mentioned in section 2.2).
- To obtain the value of $\dot{Q}_{rad}$ using the proposed simplify model (Table 2), it is critical to know the value of F_{cl}. If choosing an expression to which F_{cl} does not correspond, an approximate 35% error would be committed (in addition to the MRE reported in Table 2).
- The effect that F_{cl} can cause in $\dot{Q}_{rad}$ for F_{cl} values higher than 0.8, is not contemplated. In such cases, the roof radiative plates gain heat instead of losing.
- The use of an adjusted temperature difference $\Delta'T_{st}$, the system was modeled in an ideal way. This $\Delta'T_{st}$ value depends on the system case and meteorological data.

Conclusions

In the present work, a simplified mathematical model is wanted to be obtained to determine the nighttime radiative cooling potential from the meteorological data of a given area. First, a mathematical model was developed based on literature reviews; then, with the model's resolution, the relevant variables for the nighttime radiative cooling potential were analyzed, and our simplified mathematical model was developed based on these variables. From our study, we can conclude that the nighttime radiative cooling potential for a rainy tropical climate is appropriate to maintain thermal comfort in an enclosure when an F_{cl} is maintained within the recommended ranges; the days with the highest potential are those with lower ambient temperatures and days with low precipitation levels. In future studies, optimization methods will be implemented in order to achieve better thermal comfort performance.

Acknowledgements

Nomenclature

Variable	Symbol
Mass flow (kg/s)	$\dot{m}$
Area of the inner panel module (m^2)	A_{mc}
Outlet temperatures to the inner coil (K)	T_{ei}
Inlet temperatures to the inner coil (K)	T_{ii}
Emissivity of the radiative panel (-)	ε
Stefan-Boltzmann constant (W/m^{2}K^4)	σ
Mean radiant temperature (K)	T_{rm}
Surface temperature of the inner panel (K)	T_{si}
Convective coefficient between the interior air and panels (W/m^{2}K)	h_{ci}
Internal temperature of the enclosure (K)	T_{int}
Convective coefficient inside the coil (W/m^{2}K)	h_{coil}
Heat gained by the panels in the enclosure (W)	$\dot{Q}_{total\ enclosure}$
Heat lost by the panels on the roof (W)	$\dot{Q}_{total\ roof}$
Radiative sky cooling potential (W)	$\dot{Q}_{rad}$
Surface temperature of the exterior panel (K)	T_{st}
Outside air temperature (K)	T_{ext}
View factor of the exterior panel with respect to the sky (-)	F
Area of the exterior panel module (m^2)	A_{mt}
External convective coefficient (W/m^{2}K)	h_{ce}
Wind speed over the roof (m/s)	V_v
Sky temperature (K)	T_{sky}
Emissivity of the sky (atmospheric) (-)	ε_{sky}
Cloudiness factor (-)	F_{cl}
Emissivity for a clear sky (-)	ε_{csky}
Dew point temperature (°C)	T_{dp}
Time at which the emissivity is to be evaluated (h)	t
Atmospheric pressure (kPa)	P_{atm}

References

1. A. P. Raman, M. A. Anoma, L. Zhu, E. Rephaeli, and S. Fan, *Nature*, vol. 515, no. 7528, pp. 540–544, 2014.
2. T. E. A. Cooling, pp. 1–14, 2019.
3. A. Aili, D. Zhao, J. Lu, Y. Zhai, X. Yin, and G. Tan, *Energy Convers. Manag.*, vol. 186, no. January, pp. 586–596, 2019.
4. E. M. González, "Enfriamiento radiativo en edificaciones," 2002.
5. M. Zeyghami, D. Y. Goswami, and E. Stefanakos, *Sol. Energy Mater. Sol. Cells*, vol. 178, no. December 2017, pp. 115–128, 2018.
6. H. R. Hay and J. I. Yellott, *Sol. Energy*, vol. 12, no. 4, pp. 427–438, 1969.
7. C. I. Ezekwe, *Energy Convers. Manag.*, vol. 30, no. 4, pp. 403–408, 1990.
8. I. A. Olwi, J. A. Sabbagh, and A. M. A. Khalifa, *Sol. Energy*, vol. 48, no. 5, pp. 279–286, 1992.
9. M. Mirsadeghi, D. Cóstola, B. Blocken, and J. L. M. Hensen, *Appl. Therm. Eng.*, vol. 56, no. 1–2, pp. 134–151, 2013.
10. M. MARTIN and P. BERDAHL, *Int. J. Surg. Case Rep.*, vol. 33, 1983.